Supporting Information

Kempes et al. 10.1073/pnas.1315521110

Model for Oxygen Use Within the Colony

As described in the main text, our model is based on the combination of Monod kinetics and the Pirt model, which is a common approach in biofilm modeling (1–11). Here we provide more details for the foundation of these two perspectives and their combination into the model.

For organisms living in a continuous culture, it has been demonstrated that many species exhibit a linear relationship between their total metabolism and growth rate (12–15). The classic Pirt model (12) describes this relationship in terms of a metabolic partitioning between maintenance and growth:

$$Q = \frac{\mu}{Y_{O_2}} + P_{O_2}, \qquad \text{[S1]}$$

where Q is a consumption rate per unit mass of a limiting resource that provides energy and/or structural material to the population of cells (mol resource·s^{-1}·g $cells^{-1}$), μ is the specific growth rate (s^{-1}), Y is a yield coefficient (g cells·mol $resource^{-1}$), and P_{O_2} is a maintenance term (mol resource·s^{-1}·g $cells^{-1}$). Maintenance metabolism is defined as the consumption rate at zero growth, or the minimal requirement for survival.

The metabolic activity of a respiring population depends on the availability of an electron acceptor, such as oxygen. We add this process to Eq. **S1** by considering the dependence of growth rate on the local oxygen concentration. For *Pseudomonas aeruginosa* and many other species, growth saturates at increasing concentrations of many potentially limiting substrates, including oxygen (e.g., ref. 16). This sensitivity often is described using Monod kinetics (17):

$$\mu = \mu_{max}\frac{[O_2]}{k_{O_2} + [O_2]}, \qquad \text{[S2]}$$

where μ_{max} is the maximum growth rate approached as the substrate is taken to infinity and k_{O_2} is the half-saturation constant. Substituting Eq. **S2** into Eq. **S1** gives oxygen consumption as a saturating function of available oxygen:

$$Q = \frac{\mu_{max}}{Y_{O_2}}\frac{[O_2]}{k_{O_2} + [O_2]} + P_{O_2}. \qquad \text{[S3]}$$

As discussed in the main text, this consumption rate of oxygen, which depends on local oxygen availability, creates gradients in oxygen concentration that drive diffusion. Combining these concepts, the time-dependent spatial concentration of oxygen may be described by

$$\frac{\partial[O_2]}{\partial t} = D\nabla^2[O_2] - \left(\frac{\mu_{max}}{Y_{O_2}}\frac{[O_2]}{k_{O_2} + [O_2]} + P_{O_2}\right)a, \qquad \text{[S4]}$$

where a is the density of cells in the colony (g cells·m^{-3}). Steady state occurs when the consumption of oxygen, which depends on the local oxygen concentration via the Monod equation, balances the diffusive supply of oxygen, which is driven by gradients produced by biological consumption. It also should be noted that at zero oxygen concentration, the cells either die or become dormant; thus, we take the maintenance term P_{O_2} to be zero in the absence of oxygen. The nondimensionalization of Eq. **S4** then is given by

$$\frac{\partial[O_2]^*}{\partial t^*} = \nabla^2[O_2]^* - \left(\frac{[O_2]^*}{1 + [O_2]^*} + g\right), \qquad \text{[S5]}$$

where, again, the temporal and spatial scales, respectively, have been normalized by the factors

$$t_{fac} = \frac{a\mu_{max}}{k_{O_2}Y_{O_2}}, \quad x_{fac} = \left(\frac{a\mu_{max}}{k_{O_2}Y_{O_2}D}\right)^{1/2}, \qquad \text{[S6]}$$

oxygen concentrations have been divided by k_{O_2}, and the nondimensional maintenance term is $g = Y_{O_2}P_{O_2}/\mu_{max}$.

Model for Dual Use of Oxygen and Phenazines as Oxidants

Above and in the main text we provide a model for the metabolic response to, and the consumption of, oxygen along with its physical diffusion into and within the colony. This model, however, is appropriate only for the phenazine-null mutant (Δ*phz*), for which oxygen is the only available electron acceptor. The wild-type strain produces phenazines, which are redox active. For *P. aeruginosa*, oxidized phenazines have been shown to act as electron acceptors (18–20). When reduced phenazines are exposed to an oxidizing agent, they are thought to act as "shuttles" for electrons; that is, phenazines freely diffuse between cells, where they are reduced, and a distant electron acceptor, where they again are oxidized. Long-term anaerobic survival has been demonstrated for *P. aeruginosa* cells incubated in suspension with phenazines provided as the sole electron acceptor and an electrode poised at a potential that oxidizes the phenazines for repeated use by the cells (18). It also has been shown that the production of phenazines may help restore redox balance and reduce oxygen consumption rates as oxygen levels decrease (see Fig. 4*C* of ref. 19). Taking all these observations into consideration, we can model the oxygen consumption and reduction of phenazines as part of the redox demands of the colony in the following manner: (*i*) Oxygen freely diffuses into and within the colony and (*ii*) has two sinks: direct consumption by cells within the colony and oxidation of reduced phenazines. (*iii*) Phenazines freely diffuse within the colony in two forms, reduced and oxidized. (This is a simplification but captures the dominant first-order effects.) (*iv*) Phenazines are oxidized by oxygen according to the representative reaction

$$[Phz_r] + 2[O_2] \rightarrow [Phz_o] + 2\left[O_2^-\right]. \qquad \text{[S7]}$$

Regarding the order of kinetics for this reaction, it has been shown using pseudo-order kinetics that the exponent for phenazines should be linear (21). However, the exponent for oxygen has not, to our knowledge, been calculated, and here we leave the exponent for oxygen as a free parameter to be determined later using measurements of the colony system. Thus, we assume that oxidized phenazines are produced at a rate of $k_R[Phz_r][O_2]^{\alpha}$. (*v*) Phenazines are reduced by cells at a constant rate. This assumption follows from the observation that cells can survive but not grow on phenazines (18, 19), and within the Pirt framework (already used for oxygen consumption in Eqs. **1–3** of the main text), this is equivalent to assuming that phenazines have zero yield but can meet the minimal maintenance requirement, and thus

$$Q_{phz} = P_{phz}. \qquad \text{[S8]}$$

(*vi*) We assume that cells commit to using either oxygen or phenazines, but not both simultaneously, as an electron acceptor

because it may be costly to switch between metabolic pathways. In addition, we assume that cells have a strong preference for oxygen directly as an electron acceptor and will use oxygen unless levels are below a critical value of availability. (*vi*) We assume that the phenazine concentration within the colony is constant and that any loss terms (e.g., diffusion into and binding to the agar) are balanced by production terms (e.g., secretion by the cells). Our simulations concern the steady-state concentrations for a snapshot of the colony. On such a timescale, this balance is justified, as any production or loss dynamics would be negligible.

These processes are summarized by the following system of equations:

If $[O_2] \geq s$, then

$$\frac{\partial [O_2]}{\partial t} = D_{O_2}\nabla^2[O_2] - \left(\frac{\mu_{max}}{Y_{O_2}}\frac{[O_2]}{k_{O_2}+[O_2]} + P_{O_2}\right)a - 2k_R[Phz_r][O_2]^{\alpha} \quad \textbf{[S9]}$$

$$\frac{\partial [Phz_o]}{\partial t} = D_{phz}\nabla^2[Phz_o] + k_R[Phz_r][O_2]^{\alpha} \quad \textbf{[S10]}$$

$$\frac{\partial [Phz_r]}{\partial t} = D_{phz}\nabla^2[Phz_r] - k_R[Phz_r][O_2]^{\alpha}, \quad \textbf{[S11]}$$

if $[O_2] < s$, then

$$\frac{\partial [O_2]}{\partial t} = D_{O_2}\nabla^2[O_2] - 2k_R[Phz_r][O_2]^{\alpha} \quad \textbf{[S12]}$$

$$\frac{\partial [Phz_o]}{\partial t} = D_{phz}\nabla^2[Phz_o] - aP_{phz} + k_R[Phz_r][O_2]^{\alpha} \quad \textbf{[S13]}$$

$$\frac{\partial [Phz_r]}{\partial t} = D_{phz}\nabla^2[Phz_r] + aP_{phz} - k_R[Phz_r][O_2]^{\alpha}, \quad \textbf{[S14]}$$

where s is the minimum concentration of oxygen that can support cells; $[Phz_o]$ and $[Phz_r]$ are the concentrations of oxidized and reduced phenazines, respectively; k_R is the reaction rate coefficient for phenazine oxidation by oxygen; D again denotes the diffusivity of either oxygen or phenazines within the colony; Y and P again represent the yield coefficient and maintenance metabolism for growth on either phenazines or oxygen; and k_{O_2} and k_{phz} are the half-saturation constants for growth on oxygen and phenazines, respectively.

These equations can be nondimensionalized as:

if $[O_2] \geq s$, then

$$\frac{\partial [O_2]^*}{\partial t^*} = \nabla^{*2}[O_2]^* - \left(\frac{[O_2]^*}{1+[O_2]^*} + g_1\right) - 2R_1[Phz_r]^*[O_2]^{*\alpha} \quad \textbf{[S15]}$$

$$\frac{\partial [Phz_o]^*}{\partial t^*} = D_1\nabla^{*2}[Phz_o]^* + R_1[Phz_r]^*[O_2]^{*\alpha} \quad \textbf{[S16]}$$

$$\frac{\partial [Phz_r]^*}{\partial t^*} = D_1\nabla^{*2}[Phz_r]^* - R_1[Phz_r]^*[O_2]^{*\alpha}, \quad \textbf{[S17]}$$

if $[O_2]^* < s^*$, then

$$\frac{\partial [O_2]^*}{\partial t^*} = \nabla^{*2}[O_2]^* - 2R_1[Phz_r]^*[O_2]^{*\alpha} \quad \textbf{[S18]}$$

$$\frac{\partial [Phz_o]^*}{\partial t^*} = D_1\nabla^{*2}[Phz_o]^* - g_2 + R_1[Phz_r]^*[O_2]^{*\alpha} \quad \textbf{[S19]}$$

$$\frac{\partial [Phz_r]^*}{\partial t^*} = D_1\nabla^{*2}[Phz_r]^* + g_2 - R_1[Phz_r]^*[O_2]^{*\alpha}, \quad \textbf{[S20]}$$

where we have nondimensionalized time, spatial scales, and concentrations as

$$t^* \equiv \mathrm{t_{fac}}\,\mathrm{t} \quad \textbf{[S21]}$$

$$\{x^*, \mathrm{y}^*, \mathrm{z}^*\} \equiv x_{fac}\{x, y, z\} \quad \textbf{[S22]}$$

$$[O_2]^* \equiv [O_2]/k_{O_2} \quad \textbf{[S23]}$$

$$s^* \equiv \mathrm{s}/\mathrm{k_{O_2}} \quad \textbf{[S24]}$$

$$[Phz_o]^* \equiv [Phz_o]/k_{O_2} \quad \textbf{[S25]}$$

$$[Phz_r]^* \equiv [Phz_r]/k_{O_2} \quad \textbf{[S26]}$$

with

$$t_{fac} \equiv \frac{a\mu_{max}}{k_{O_2}Y_{O_2}} \quad \textbf{[S27]}$$

$$x_{fac} \equiv \left(\frac{a\mu_{max}}{k_{O_2}Y_{O_2}D_{O_2}}\right)^{1/2} = \left(\frac{t_{fac}}{D_{O_2}}\right)^{1/2} \quad \textbf{[S28]}$$

$$g_1 \equiv \frac{Y_{O_2}P_{O_2}}{\mu_{max}} \quad \textbf{[S29]}$$

$$g_2 \equiv \frac{Y_{O_2}P_{phz}}{\mu_{max}} \quad \textbf{[S30]}$$

$$D_1 \equiv \frac{D_{phz}}{D_{O_2}} \quad \textbf{[S31]}$$

$$R_1 \equiv \frac{k_R k_{O_2}^{\alpha+1} Y_{O_2}}{a\mu_{max}}. \quad \textbf{[S32]}$$

Parameter Values of the Mathematical Models

Many of the key parameters from our model for oxygen consumption and/or phenazine reduction can be estimated from earlier studies (19, 21).

Using the data from figure 4A of ref. 19, we calculate growth rate as a function of oxygen concentration and determine the Monod kinetics for oxygen-limited growth. We calculate the specific growth rate according to $\mu = d\ln(\mathrm{OD})/dt$, and we convert oxygen percentages to concentration by multiplying by the saturation concentration of oxygen in water. We find that the maximum growth rate is $\mu_{max} = 2.27 \times 10^{-4}$ (divisions s^{-1}) and that the half-saturation constant is $k_{O_2} = 0.0124$ (mol $\mathrm{O_2}{\cdot}\mathrm{m}^{-3}$).

Using figure 2 of ref. 19, which provides a time series for both optical density and phenazine reduction rates by cells in liquid culture, we calculate the maintenance coefficient for survival on phenazines. We used the reduction rates to calculate Q_{phz}, the phenazine consumption rate per gram of cell (mol $\mathrm{Phz_o}{\cdot}\mathrm{g}^{-1}{\cdot}\mathrm{s}^{-1}$), by noting that the sample volume is 1 mL and using the conversions found below. Under our assumptions for phenazine consumption, this is equivalent to the maintenance coefficient. We make these calculations for the data at 27 h, as this corresponds to the maximum phenazine reduction rate reached after

the culture has entered stationary phase. We estimate that $P_{phz} = 5.03 \times 10^{-7}$ (mol Phz_o·g cells^{-1}·s^{-1}), which is roughly four times larger than the value for O_2.

The oxidizing reaction rate of reduced phenazines and oxygen may be calculated using the data in ref. 21 and solving for $k_R = R_o/([Phz_r][O_2]^{\alpha})$, where R_o is the observed oxidation rate. We have that for 0.005 (mol·m^{-3}) of phenazines and roughly 0.022 (mol·m^{-3}) of oxygen (2% oxygen) that the reaction rate for pyocyanin is 1.75×10^{-5} (mol·m^{-3}·s^{-1}), and thus $k_R = 1.75 \times 10^{-5}/(0.005 \times 0.22^{\alpha})$ (mol^{-2}·m^{-3}·s^{-1}).

The critical value for O_2 consumption, s, can be estimated from figure 4C of ref. 19. It is observed that as oxygen levels are drawn down, there is a sudden increase in the production of phenazines. Following the increase in phenazine production, oxygen levels are observed to rise in the culture, indicating that oxygen consumption has been reduced and that some of the cells have started using phenazines rather than oxygen. These transitions occur for a concentration $s \sim 0.0087$ (mol O_2·m^{-3}), which may be interpreted as the critical oxygen concentration determining whether wild-type cells are using oxygen or phenazines. It should be noted that in ref. 19, our estimate for s also corresponds to the maximum redox imbalance (as measured by the ratio of NADH and NAD^+ values), and after phenazine production increases, this redox imbalance decreases. These observations agree with the perspective that s is the critical concentration at which cells respond by producing phenazines and switching between electron acceptors.

Finally, the total pool of phenazines within the colony is estimated from figure 4C of ref. 19. We use the maximum concentration of pyocyanin, 0.27 (mol·m^{-3}), as the concentration in the colony biofilm. It is possible that this value should be scaled by differences in density of cells in the liquid culture compared with the colony, but we find that measurements of pyocyanin concentration in the biofilm and agar are comparable to the concentration in liquid culture. We take $D_1 = .3$, which agrees with empirical observations.

Many parameters of our model, such as the maximum growth rate μ_{max}, often are measured in the literature. Thus, for comparison with our calculated values, we searched the literature for reasonable ranges of these parameters as summarized in Table S1. When we nondimensionalize the mathematical model, all these parameters are summarized by three normalization factors and one dimensionless parameter: x_{fac}, t_{fac}, k_{O_2}, $g1$, $g2$, $D1$, and $R1$. Each of these terms is determined by a combination of the underlying parameters. To obtain a best estimate for each factor, we first calculated each factor from every combination of measured parameter values (Table S1), then found the mean of all of the combinations. Doing this, we find that the mean value of x_{fac} is 76,542.9 s^{-1}. The mean estimate for g is 0.012. Note that t_{fac} is not critical to the analysis in which we examine steady states, but it may be found easily from the parameters presented here.

Converting Between Optical Density and Mass Units

In ref. 27, the conversion between OD and cfu per cubic meter is given by

$$\text{cfu/m}^3 = (2.0 \times 10^{14})\,\text{OD} + 4.0 \times 10^{12}. \quad \textbf{[S33]}$$

Similarly, taking the average of the reviewed literature in ref. 27, the mass per number of cells is $2.14 \pm 3.9 \times 10^{-12}$ (g per cell), which implies that the conversion between OD and grams per cubic meter is given by

$$\text{g/m}^3 = 428.3\ \text{OD} + 8.6. \quad \textbf{[S34]}$$

Modeling Approach

To determine the spatial distribution of oxygen in the Δ*phz* colony, we numerically solved Eq. **3** from the main text for 2D wrinkles (one vertical dimension and one horizontal dimension). We held the colony surface to a constant value of atmospheric oxygen concentration and used circular horizontal boundary conditions to represent the repeating pattern of wrinkles that emanate outward from the center of the colony. We used an explicit second-order Runge–Kutta finite difference method for the numerical solutions.

For the geometry of biofilm features, we use a "Gaussian" shape with an elliptical tip, in which we adjust the width of the base to match cross-sections of the colony wrinkles given the observed height of these wrinkles. We found that various mathematical forms that approximate the shape of the wrinkles do not alter our results significantly.

Steady-state solutions for the profiles of oxygen and phenazines in the wild-type colonies are solved by using Eqs. **S17–S24**, using the same numerical techniques described above. It should be noted that each model may be used within either a 1D or 2D context. For example, the Δ*phz* model is used in a 1D context to solve for the ideal base thickness, whereas the optimal wrinkle width is found using the full 2D geometry of the wrinkle, as described above and in the next section.

Geometric Effects on Oxygen Availability and Colony Growth

Our model can capture the decrease in oxygen availability with increasing depth into the colony, and we find that this decay rate is controlled largely by local geometry. For example, the wrinkles have a much deeper penetration depth of oxygen resulting from increased local surface area per unit of cellular mass. As discussed in the main text, we have observed that wrinkles reach a constant width while growing taller and that this width is sensitive to the availability of oxygen (and the presence or absence of phenazines). To interpret this phenomenon, and the significance of geometry, we simulate the steady-state distribution of oxygen availability within a wrinkle and the surrounding base for various geometries of the wrinkle (Fig. S3*A*). From the distribution of oxygen availability within the colony, we also can calculate the spatial distribution of growth rates (Fig. S3*B*). It is from these results that we calculate the total growth rate of the colony as a function of wrinkle width and find that there is a wrinkle width that optimizes colony growth per mass investment.

Model Calibration and Metabolic Observations

In the main text, we used measured profiles of the oxygen concentration as a function of depth into the colony to verify our model and compare parameter values to our estimate from the literature. Fig. S1 provides all the measured profiles for both the base and wrinkle regions of Δ*phz* grown in 21% external oxygen. These data also were used for analysis in ref. 20. Similarly, Fig. S2 shows all the wild-type oxygen profiles for the base grown in 40% oxygen.

Ref. 20 provides measurements for constitutively expressed YFP in the base regions of wild type and the Δ*phz* mutant. The YFP signal can be interpreted as a proxy for some aspect of overall metabolic activity (protein expression). In the Δ*phz* mutant oxygen availability, base thickness, and the expression of YFP coincide. In contrast, a wild-type base is significantly thicker than the distance oxygen can penetrate into the colony, creating an oxic and apparent anoxic zone. Interestingly, YFP expression extends into the anoxic zone (YFP expressed in the anoxic zone matures and fluoresces after the thin section is exposed to oxygen, post fixation). We find that the thickness of the base corresponds to the optimum for cellular reproduction, and the levels of YFP in the wild type that extend deeper than oxygen

indicate that cells are at least meeting their maintenance requirement at these depths. Thus, the depth at which oxygen is no longer detectable cannot simply be that at which growth ceases but instead should be considered as the site of a transition in metabolic activity. Using our wild-type model (calibrated by oxygen profiles) we solve for the depth at which phenazines are no longer able to support basic maintenance requirements and we predict that this depth should be 103.7 μm for 21% external oxygen. This prediction compares well with the measured YFP depth of 99.1 ± 15.0 (20). This analysis supports our treatment of metabolic switching and the value for s and provides another avenue for model calibration using the YFP signals.

Thus, experimental data from reference (20) allowed us to calibrate oxygen and phenazine parameters. Base oxygen profiles verified the simulated oxygen profile for both wild-type and Δ*phz* colonies. The maximum YFP depth verified the wild-type phenazine profile given that we interpret this depth to correspond to the point at which oxidized phenazine concentrations can no longer support the basic maintenance requirement of the cells. Our free parameter of the phenazine model (compared to x_{fac} for oxygen) is the exponent for oxygen, α, in the phenazine oxidation rate equation. We find that for $\alpha = 1$ our model matches the oxygen profiles and the depth at which oxidized phenazines are negligible compares well to the maximum depth at which YFP is detectable.

For situations where we do not have the appropriate experimental setup to directly measure oxygen profiles in Δ*phz* (40% or 15% external oxygen) we used total base thickness or the YFP depth, both proxies for the depth at which oxygen is no longer detectable, to calibrate the modeled oxygen profiles. The minimum base thickness in 40% oxygen is 98.2 μm, the maximum is 169.8 μm, and the mean is 138.8 ± 27.2 μm where the error represents the standard deviation.

For all the base calculations, we find solutions of the Δ*phz* and wild-type models in one dimension in which we enforce a no-flux boundary condition at the agar and hold the surface of the base to atmospheric oxygen concentrations. (For the Δ*phz* model, no-flux boundary conditions are imposed for phenazines at all surfaces.) This is equivalent to a base extending infinitely in all directions and is a good approximation for the base region between wrinkles, as the wrinkles do not alter the chemical concentrations in the base region beyond a distance of roughly 40 μm (Fig. S3). The optimal base thickness may be found by observing the saturation in the total growth R as a function of base thickness.

Predictions for Geometry in Δ*phz* Colonies Grown in 15% External Oxygen

In the main text, we provide our predictions for the wrinkle widths of Δ*phz* grown in 21% and 40% external oxygen. Fig. S4 gives our predictions for wrinkles grown in 15% oxygen. We find that in this condition, wrinkles are narrower compared with 21% external oxygen conditions. Our results show that wrinkles will respond to external oxygen by becoming thicker in elevated (40%) oxygen conditions and narrower in lower oxygen conditions (15%). The reduced oxygen conditions are important for understanding the response of the biofilm to common hypoxic environments.

Predictions for Geometry in Wild-Type Colonies Grown in 21% External Oxygen

Fig. 3*D* in the main text provides our predictions for the optimal width of wrinkles in the wild-type biofilm. These were found using Eqs. **S17**–**S24**. In our analysis of the Δ*phz* system, we found that optimizing growth for a 1D plate of different thicknesses gave approximately the same predicted width as the full 2D solution within the wrinkle geometry. This 1D setup is equivalent to an infinitely tall ridge with both sides held to atmospheric oxygen concentration. We found a simple scaling factor, of roughly 1.1, relating the 1D prediction to the full 2D prediction. For the wild-type predictions, we solve Eqs. **S17**–**S24** in one dimension and multiply by this same scaling factor.

1. Sinsabaugh RL, Follstad Shah JJ (2012) Ecoenzymatic stoichiometry and ecological theory. *Annu Rev Ecol Evol Syst* 43:313–343.
2. Kondo S, Miura T (2010) Reaction-diffusion model as a framework for understanding biological pattern formation. *Science* 329(5999):1616–1620.
3. Murray J (2002) *Mathematical Biology: An Introduction* (Springer, Berlin).
4. Mimura M, Sakaguchi H, Matsushita M (2000) Reaction–diffusion modelling of bacterial colony patterns. *Physica A* 282(1):283–303.
5. Stewart PS (2003) Diffusion in biofilms. *J Bacteriol* 185(5):1485–1491.
6. Klapper I, Dockery J (2010) Mathematical description of microbial biofilms. *SIAM Rev* 52(2):221–265.
7. Kreft JU, Picioreanu C, Wimpenny JW, van Loosdrecht MC (2001) Individual-based modelling of biofilms. *Microbiology* 147(11):2897–2912.
8. Petroff AP, et al. (2011) Reaction-diffusion model of nutrient uptake in a biofilm: Theory and experiment. *J Theor Biol* 289:90–95.
9. van Loosdrecht MC, Heijnen JJ, Eberl H, Kreft J, Picioreanu C (2002) Mathematical modelling of biofilm structures. *Antonie van Leeuwenhoek* 81(1-4):245–256.
10. Golding I, Kozlovsky Y, Cohen I, Ben-Jacob E (1998) Studies of bacterial branching growth using reaction–diffusion models for colonial development. *Physica A* 260(3): 510–554.
11. Benefield L, Molz F (1985) Mathematical simulation of a biofilm process. *Biotechnol Bioeng* 27(7):921–931.
12. Pirt SJ (1965) The maintenance energy of bacteria in growing cultures. *Proc R Soc Lond B Biol Sci* 163(991):224–231.
13. Farmer IS, Jones CW (1976) The energetics of Escherichia coli during aerobic growth in continuous culture. *Eur J Biochem* 67(1):115–122.
14. Shepherd MG, Sullivan PA (1976) The production and growth characteristics of yeast and mycelial forms of Candida albicans in continuous culture. *J Gen Microbiol* 93(2): 361–370.
15. Lee Y, Pirt S (1981) Energetics of photosynthetic algal growth: Influence of intermittent illumination in short (40 s) cycles. *Microbiology* 124(1):43.
16. Alagappan G, Cowan RM (2004) Effect of temperature and dissolved oxygen on the growth kinetics of Pseudomonas putida F1 growing on benzene and toluene. *Chemosphere* 54(8):1255–1265.
17. Monod J (1949) The growth of bacterial cultures. *Annu Rev Microbiol* 3:371–394.
18. Wang Y, Kern SE, Newman DK (2010) Endogenous phenazine antibiotics promote anaerobic survival of Pseudomonas aeruginosa via extracellular electron transfer. *J Bacteriol* 192(1):365–369.
19. Price-Whelan A, Dietrich LE, Newman DK (2007) Pyocyanin alters redox homeostasis and carbon flux through central metabolic pathways in Pseudomonas aeruginosa PA14. *J Bacteriol* 189(17):6372–6381.
20. Dietrich L, et al. (2013) Bacterial community morphogenesis is intimately linked to the intracellular redox state. *J Bacteriol* 195(7):1371–1380.
21. Wang Y, Newman DK (2008) Redox reactions of phenazine antibiotics with ferric (hydr)oxides and molecular oxygen. *Environ Sci Technol* 42(7):2380–2386.
22. Lewandowski Z, Walser G, Characklis WG (1991) Reaction kinetics in biofilms. *Biotechnol Bioeng* 38(8):877–882.
23. Strand S, McDonnell A (1985) Mathematical analysis of oxygen and nitrate consumption in deep microbial films. *Water Res* 19(3):345–352.
24. Beyenal H, Chen S, Lewandowski Z (2003) The double substrate growth kinetics of Pseudomonas aeruginosa. *Enzyme Microb Technol* 32(1):92–98.
25. Bakke R, Trulear MG, Robinson JA, Characklis WG (1984) Activity of Pseudomonas aeruginosa in biofilms: Steady state. *Biotechnol Bioeng* 26(12):1418–1424.
26. Shreve GS, Vogel TM (1993) Comparison of substrate utilization and growth kinetics between immobilized and suspended Pseudomonas cells. *Biotechnol Bioeng* 41(3): 370–379.
27. Kim DJ, Chung SG, Lee SH, Choi JW (2012) Relation of microbial biomass to counting units for Pseudomonas aeruginosa. *Afr J Microbiol Res* 6(21):4620–4622.

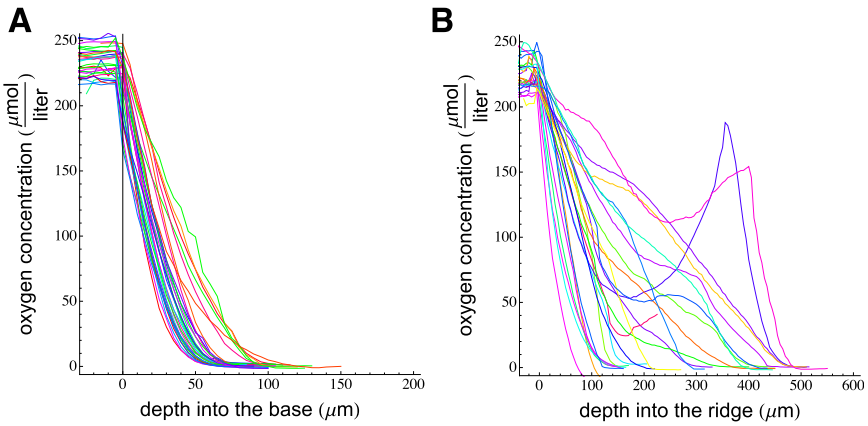

Fig. S1. All the measured oxygen profiles for the base region (*A*) and wrinkles (*B*) of Δ*phz* colonies grown in 21% external oxygen. Note that the wide range of wrinkle profile decay rates, as well as the occasional increase in oxygen with increasing depth, is a result of the thin geometry of the wrinkle and the resulting experimental challenge of keeping the oxygen probe centered in the wrinkle as it moves deeper into the colony. Data from ref. 20.

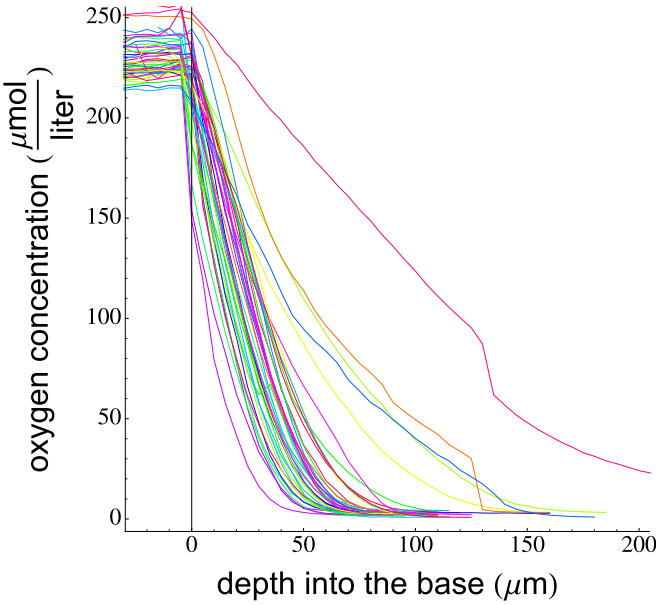

Fig. S2. All the measured oxygen profiles for the base region of wild-type colonies grown in 40% oxygen. Data from ref. 20.

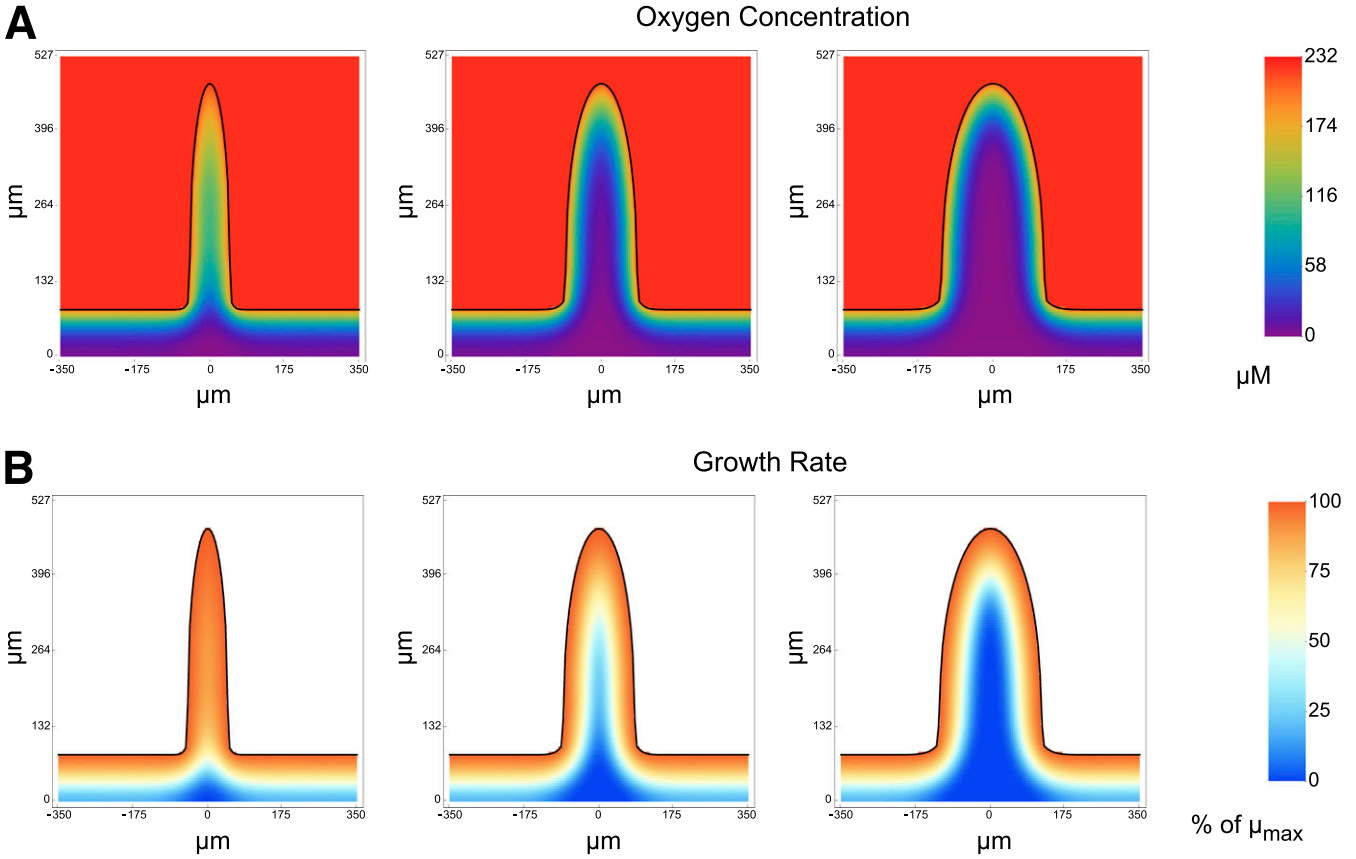

Fig. S3. The modeled internal availability of oxygen (*A*) along with the spatial distribution of growth rate (*B*) within a biofilm for features of different sizes.

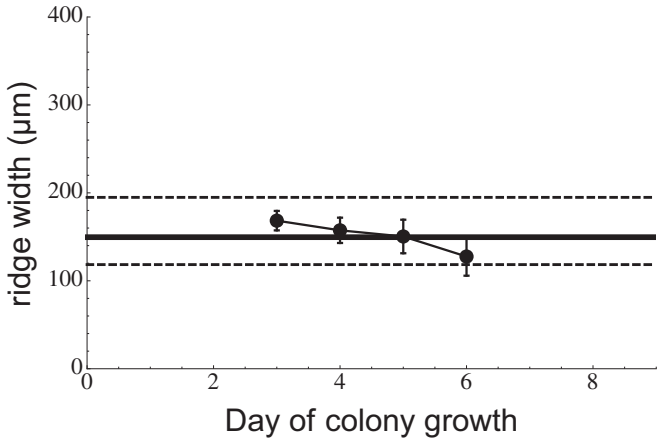

Fig. S4. The average width (points) of Δ*phz* colony wrinkles grown in 15% external oxygen as a function of time. The solid line represents our predictions for optimal wrinkle width, and the dashed lines are our predictions for the bounds of variation in wrinkle width. The data were published previously in ref. 20.

Table S1. Reported values for key biological and physical parameters

Parameter (symbol)	Value	Ref.
Half-saturation constant (k_{O_2}), mol $O_2 \cdot m^{-3}$	**0.0124**	(**19**)
	0.0078	(22)
	0.0014	(23)
	0.0125	(24)
	0.0369	(24)
Maximum growth rate (μ_{max}), s^{-1}	**2.27×10^{-4}**	(**19**)
	1.11×10^{-4}	(25)
	7.89×10^{-5}	(26)
	2.78×10^{-5}	(26)
	6.11×10^{-5}	(23)
	5.28×10^{-5}	(24)
	8.89×10^{-5}	(24)
	2.22×10^{-4}	(5)
Yield coefficient for O_2 (Y_{O_2}), g cells·mol O_2^{-1}	20.80	(23)
	27.20	(5)
	20.32	(24)
Maintenance coefficient for O_2 (P_{O_2}), mol O_2·g $cells^{-1} \cdot s^{-1}$	1.22×10^{-7}	(24)
Maintenance coefficient for phenazines (P_{phz}), mol Phz_o·g $cells^{-1} \cdot s^{-1}$	5.03×10^{-7}	(19)
Oxidation rate for phenazines by O_2 (k_R), $mol^{-2} \cdot m^{-3} \cdot s^{-1}$	0.16	(21)
Diffusivity for O_2 in the colony (D_{O_2}), $m^2 \cdot s^{-1}$	1.76×10^{-9}	(22)
	1.53×10^{-9}	(5)
Biofilm cell density (a), g $cells \cdot m^{-3}$	12,000	(5)
Critical value of oxygen (s), mol $O_2 \cdot m^{-3}$	0.0087	(19)

Bold text indicates situations in which we used a value calculated here rather than the average of the published values.